

Characterization of stain-etched porous silicon

S. Liu, C. Palsule, S. Yi, and S. Gangopadhyay

Department of Physics, Texas Tech University, Lubbock, Texas 79409

(Received 25 October 1993; revised manuscript received 13 December 1993)

We have performed infrared absorption, continuous-wave photoluminescence, and nanosecond photoluminescence decay measurements to characterize stain-etched porous silicon. Stain-etched porous silicon samples were prepared by etching boron-doped crystalline silicon wafers in a solution of HF:HNO₃:H₂O with ratios of 1:5:10 by volume. The dependence of continuous-wave photoluminescence intensity upon temperature and excitation energy has been studied. We have also investigated the dependence of nanosecond photoluminescence decay upon temperature, excitation energy, and emission energy. Our results suggest that the photoluminescence in stain-etched porous silicon might be due to the presence of siloxene-type bonding configuration in an amorphous alloy of silicon, oxygen, and hydrogen.

I. INTRODUCTION

Porous silicon (*p*-Si) from anodic etching was reported by Canham¹ to exhibit visible photoluminescence (PL) at room temperature. This discovery has stimulated a significant amount of research on this material²⁻⁵ in order to understand its structure, composition, and the origin of its PL. Although most of the work has concentrated on *p*-Si prepared using anodic etching, Fathauer *et al.*⁶ have reported that simple stain etching of Si wafers in HF:HNO₃:H₂O solution produces films which exhibit visible room-temperature luminescence similar to that of *p*-Si formed by anodic etching followed by chemical dissolution. This result is important from a technological point of view, because stain-etched films are much easier to produce, requiring no special equipment.

The stain-etched *p*-Si has been characterized in the past using cross-sectional transmission electron microscopy,⁶ continuous-wave (cw) PL,⁶ and x-ray photoelectron spectroscopy.⁷ In this paper, we present our results on infrared (ir) absorption spectroscopy, cw PL, and nanosecond PL decay in stained-etched *p*-Si films. Our results seem to support the idea that the origin of PL in stain-etched *p*-Si is due to the presence of a siloxene (Si₆O₃H₆) type of bonding configuration in an amorphous alloy of silicon, oxygen, and hydrogen.

II. EXPERIMENTAL METHOD AND DATA ANALYSIS

The *p*-Si samples were prepared by etching boron-doped crystalline silicon wafer (111) with 30–40 Ω cm resistivity in a solution of HF:HNO₃:H₂O with ratios of 1:5:10 by volume.⁶ Reagents used were standard electronic-grade 49% HF, 70–71% HNO₃, and deionized water. The as-prepared stain-etched *p*-Si films appear brown, blue, and golden with different etching times, consistent with that described by Fathauer *et al.*⁶ After etching, the samples were rinsed with deionized water and stored in the dark in a helium atmosphere to avoid degradation due to air and light exposure. The stain-etched films luminesce bright red to orange to the naked eye at room temperature under ultraviolet irradiation

(363 nm). The ir absorption spectra of the samples were recorded in a nitrogen ambient using a model 1600 Perkin-Elmer spectrometer.

For PL measurements, the *p*-Si samples were housed in a closed-cycle refrigeration system, where the temperature could be varied between 25 and 475 K. A xenon lamp with 456-nm bandpass filter and a 632-nm helium-neon laser line were used as the excitation sources for cw PL measurements. The PL signal was dispersed with a SPEX double monochromator and detected by a photomultiplier tube (PMT). For cw measurements, an infrared-sensitive Hamamatsu In_xGa_{1-x}As side-on PMT was used. cw data from the PMT were recorded with a Keithly picoammeter and an IBM PC. All the cw spectra were corrected for the instrument spectral response. The PL decay measurements were carried out using a N₂-pumped dye laser. The excitation wavelengths were 373 and 540 nm. The laser pulses were 500 ps wide and delivered 100–150 μJ per pulse at rates up to 20 Hz. The PL decays were recorded in the range of 500–700 nm depending on the excitation. Due to low sensitivity of the multichannel-plate MCP PMT in the infrared region, we were not able to detect PL decays below 700 nm. Suitable cutoff filters were used to eliminate excitation light scattered off the surface of the sample. The PL decays were detected with a Hamamatsu two-stage proximity-focused multichannel-plate photomultiplier tube. The output from the MCP PMT was directed to a Tektronix wave-form digitizer and the signal was averaged over a number of pulses using an IBM PC. The data analysis was performed on a VAX 8650 mainframe computer.

The measured PL decay signal $M(t)$ is the convolution of the actual PL decay with the temporal instrument response. In order to obtain the actual PL decay, an iterative deconvolution technique and least-squares fitting are used.⁸ To determine the number of components present in the decay, the PL decays are first fitted with an exponential-series⁹ method. This method requires no previous knowledge or assumptions about the underlying distribution. The analysis is performed by assuming that a set of fixed lifetimes and an associated set of variable pre-exponential factors may be used to fit the PL decay

curve. From the best fit, a plot of the relative contribution of a lifetime can be plotted against the lifetime, yielding the lifetime distribution. In this work the data were fitted with a distribution of 20–40 decay times in the range of 0.1 to 50 ns. From the number of peaks in the lifetime distribution, the number of decay times can be obtained. More details of the data analysis are presented elsewhere.⁸

III. RESULTS AND INTERPRETATION

A. ir absorption

The ir absorption spectra for *p*-Si were obtained by correcting for the substrate absorption. Figures 1(a), 1(b),

and 1(c) show the ir absorption spectra of stain-etched *p*-Si in the 500–800, 800–1200, and 2000–2300 cm^{-1} regions, respectively. For comparison, we have also plotted the ir absorption spectra of an anodically etched sample (*p*-type crystalline silicon, HF:ethanol 3:7, current density 10 mA/cm^2 , etching time 20 min) after correcting for substrate absorption. The ir spectrum of the anodically etched sample is similar to that reported in the literature^{3,10,11} with peaks at 628, 665, 906, 2087, 2100, and 2143 cm^{-1} . As can be seen from Figs. 1(a), 1(b), and 1(c), the ir spectrum for stain-etched *p*-Si also shows all these peaks, but the relative intensities of the peaks are different from the anodically etched sample. In the case of the anodically etched sample, two dominant peaks are present at 665 and 628 cm^{-1} , whereas in stain-etched

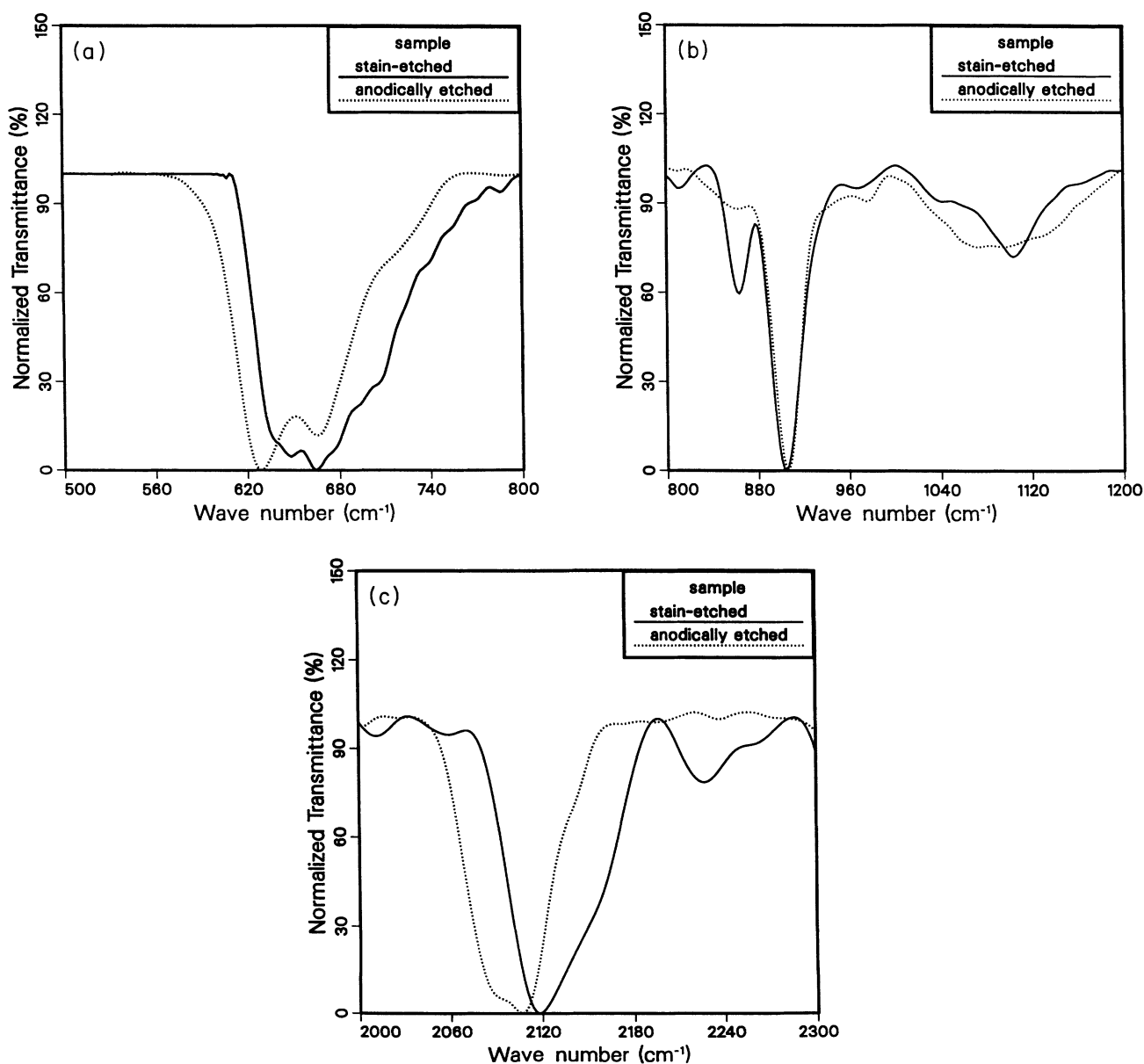


FIG. 1. Fourier-transformed ir spectra of stain-etched and anodically etched porous silicon films: (a) 500–800 cm^{-1} , (b) 800–1200 cm^{-1} , and (c) 2000–2300 cm^{-1} . For comparison the spectra have been normalized at the peak.

samples, the 665-cm^{-1} peak dominates and the 628-cm^{-1} peak appears as a shoulder. The position of the 628-cm^{-1} peak is dependent on the correction of the ir spectrum for substrate absorption. Without the correction, the position of this peak has been reported^{10,11} to be $611\text{--}617\text{ cm}^{-1}$. This peak is generally assigned to the Si-Si stretching mode¹¹ and the 665-cm^{-1} peak is assigned to the Si-H wagging¹¹ mode. The stain-etched *p*-Si shows an additional peak at 705 cm^{-1} which we assign to the O-Si-O bending mode.¹² The peak at 906 cm^{-1} due to the Si-H₂ scissor-mode vibration is present in both the samples. The additional peak in stain-etched *p*-Si at 860 cm^{-1} can be attributed to the Si-H₂ wagging mode, shifted to higher frequencies due to the presence of oxygen. Both the samples show a broad absorption band in the $1000\text{--}1200\text{-cm}^{-1}$ region, which is generally assigned to the Si-O-Si asymmetric stretch. In the anodically etched sample, the band in the $2000\text{--}2200\text{-cm}^{-1}$ region is dominated by Si-H₂ (2087 cm^{-1}) and Si-H (2100 cm^{-1}) stretching-mode absorption. There is a small shoulder at 2143 cm^{-1} which is attributed to the substitution of oxygen into the backbones of the Si-H stretch.¹⁰ In stain-etched samples, the band in the $2000\text{--}2200\text{-cm}^{-1}$ region is dominated by absorptions at 2117 cm^{-1} (Si-H stretch) and 2145 cm^{-1} . The Si-H₂ stretching mode (2085 cm^{-1}) appears only as a small shoulder. In addition, the stain-etched film shows a peak at 2240 cm^{-1} which we assign to O-Si-H stretching.³ The samples etched for different durations (up to 1 h) do not show any observable change in the position of the peaks in the ir spectra, but the area under the oxygen-related peaks ($1000\text{--}1200\text{ cm}^{-1}$, 2240 cm^{-1}) decreases with increase in etching time. This suggests that with an increase in etching time the oxygen concentration in the films decreases, probably due to better hydrogenation by HF. The assignments of all the peaks in stain-etched *p*-Si match very closely to the peaks reported in the ir absorption spectra of siloxene molecules¹³ except for the O-H stretch (3450 cm^{-1}), which is missing in our spectra. We do see the O-H stretch in films that are left exposed to air for a few days. According to Brandt *et al.*³ there are three possible structural phases of siloxene. Of these three possible phases, only one has substantial direct O-H bonding. So it is possible that *p*-Si contains bonding which is characteristic of the other two structures, in which the Si-O-Si and H-Si-O types of bonding are more prevalent; these show up in our ir absorption spectra.

B. cw photoluminescence

The average quantum efficiency of stain-etched films is lower than that of anodically etched films. A part of the reason may be the thickness of the films, but a major part may be their structural composition. Figures 2(a) and 2(b) show the cw PL spectra of stain-etched *p*-Si with 456- and 632-nm excitation at different temperatures from 25 to 250 K. At 25 K with 456-nm excitation, a broad luminescence band with a peak at 730 nm (1.70 eV) and a full width at half maximum (FWHM) of about 0.40 eV was observed. Up to 75 K, there was no change in PL intensity with temperature. Above 75 K, there was weak

thermal quenching and a blueshift in PL. With 632-nm excitation, the luminescence peak shifted to 780 nm (1.59 eV) and the FWHM was about 0.28 eV. In this case also the PL intensity was constant up to 75 K, and above 75 K there was strong thermal quenching with negligible shift in the PL spectra. From these observations we suggest that there are two components in the PL spectrum obtained with high-energy excitation [see Fig. 2(a)], while the PL spectrum obtained with low-energy excitation [see Fig. 2(b)] consists of only one component. The two components present in the PL spectrum obtained with high-energy excitation have different origins and hence different temperature dependencies. In order to separate the two components, we fitted the spectra in Fig. 2(a)

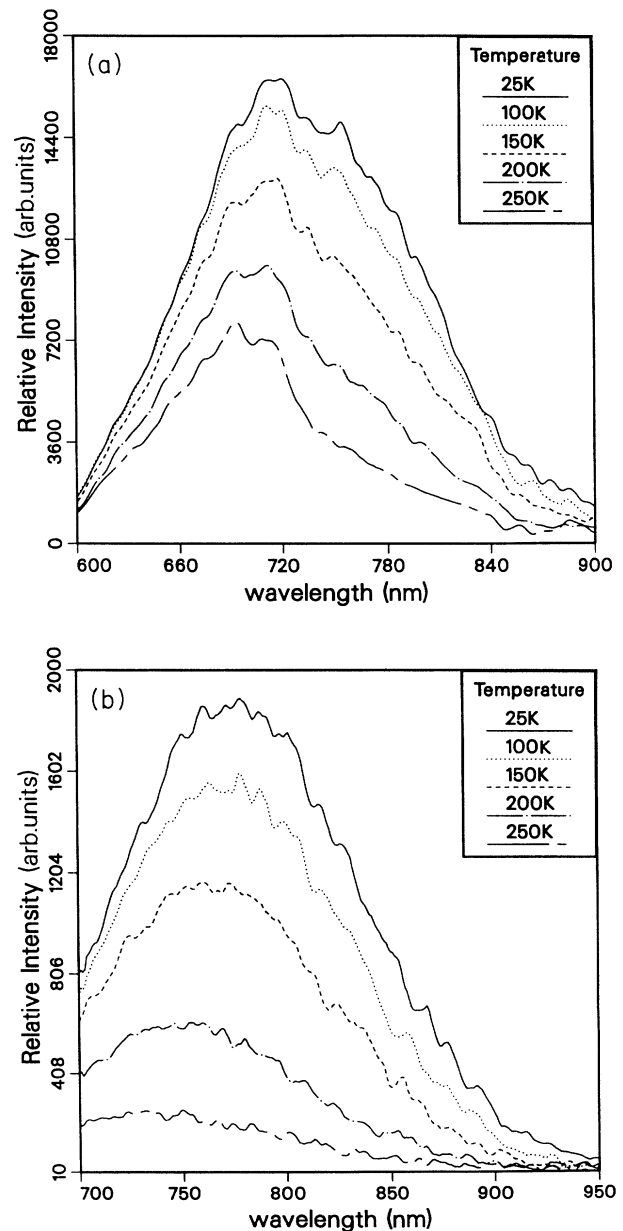


FIG. 2. cw PL spectra of stain-etched *p*-Si with (a) 456-nm excitation and (b) 632-nm excitation at different temperatures from 25 to 250 K.

with a sum of two Gaussians. Figure 3 shows the two resolved components at 25 K with peaks at 700 and 780 nm, respectively. A similar fit with a sum of two Gaussians for the entire temperature range yields two components with PL peaks at 700 ± 4 and 780 ± 5 nm with FWHM of 0.33 and 0.2 eV, respectively. The peak position for the second component is the same as the peak position obtained by low-energy excitation, which suggests that these two bands have the same origin. It is interesting to note that the two types of siloxenes prepared with different techniques (namely, the Kautsky method¹⁴ and the Wöhler method¹⁵) and annealed at 400 °C result in PL peaks at 690 and 760 nm, respectively.³ The similarity of these two peak positions to the peak positions of the two components that we found with high-energy excitation is remarkable, and supports the presence of a mixture of different structural phases of siloxene in *p*-Si. The PL intensities of the spectra in Figs. 2(a) and 2(b) suggest that 2.71-eV excitation is much more efficient than 1.96-eV excitation as far as exciting luminescence in the red spectral region is concerned. This result agrees well with the earlier results on *p*-Si,^{3,16} and with calculations based on siloxene compounds.¹⁷

From the study of the temperature dependence of the PL intensity of *p*-Si, an activation energy of 60 ± 15 meV has been reported¹⁸ for temperatures above 100 K. Our results indicate that the temperature dependence of the integrated PL intensity for neither of the two components can be fitted with a single activation energy, but we can fit our data with another model which is frequently used to explain the temperature dependence of PL in chalcogenide glasses¹⁹ and amorphous silicon alloys.²⁰ The functional form of this model is given by

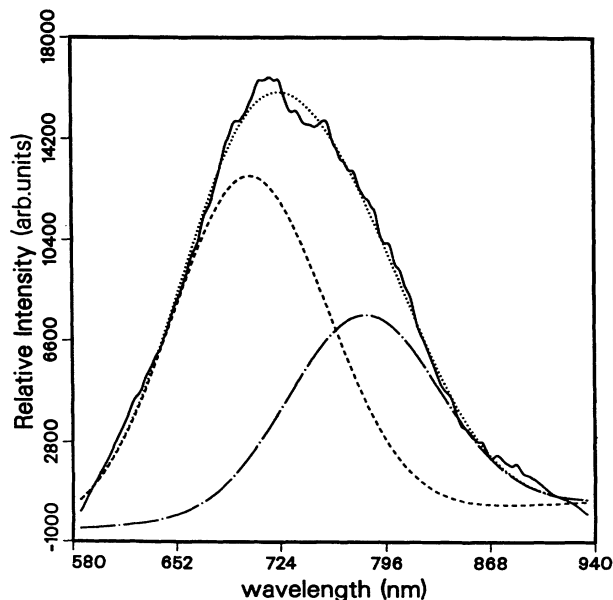


FIG. 3. Resolution of the two components of the cw PL spectrum at 25 K with 456-nm excitation by fitting with a sum of two Gaussians. The solid line is the raw spectrum and the dotted line is the fit. The two resolved components are also shown.

$$\frac{1}{I(T)} = 1 + I(0)\exp(T/T_0), \quad (1)$$

where $I(T)$ is the integrated PL intensity, and $I(0)$ and T_0 are fitting parameters. In Fig. 4, curve *a* and curve *b* show the plot of $1/I(T)$ versus temperature for the two components obtained by resolving the PL spectrum obtained using high-energy excitation. Curve *c* is a similar plot with 632-nm excitation. The lines represent the best fits of Eq. (1) to the data. All our fits are in excellent agreement with Eq. (1), and the values of the parameter T_0 are determined to be 71.3 ± 8.9 , 47.5 ± 0.8 , and 46.5 ± 0.5 K for the curves *a*, *b*, and *c* shown in Fig. 4, respectively. A comparison of the fitting parameters for the curves *b* and *c* shows that they have the same temperature dependence of cw PL intensity, supporting the conclusion that they have the same origin. For anodically etched *p*-Si the characteristic temperature (T_0) of 50 K has been reported by Stutzmann *et al.*,¹³ but they did not separate the PL spectrum into two components as in this work. The functional form of the temperature dependence of the integrated PL intensity is similar to that exhibited by siloxene, but the value of T_0 is smaller than that reported for siloxene.²¹ These values of T_0 are higher than those reported for intrinsic *a*-Si:H,²⁰ but they are comparable to those for alloys like *a*-Si:O:H and *a*-Si:C:H. As a result, we cannot exclude the possibility that a part of the *p*-Si is actually an alloy like *a*-Si:O:H. With the different temperature dependences of the two components of the PL spectrum, it is easy to explain the

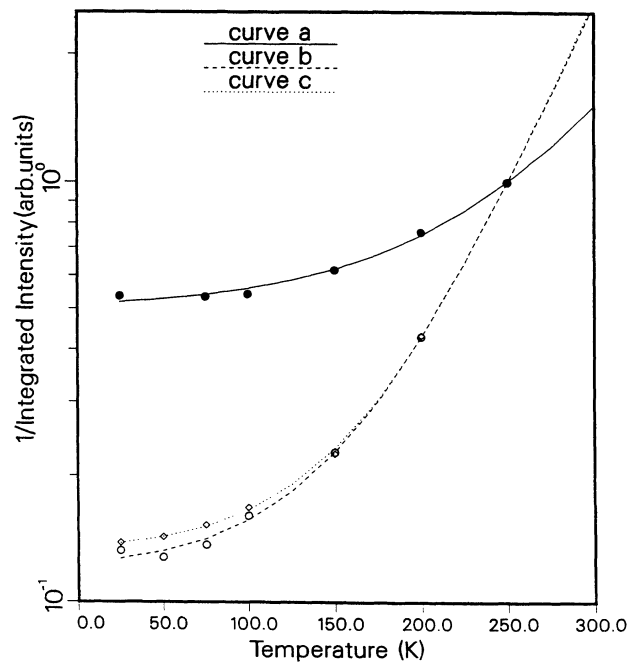


FIG. 4. $1/I(T)$ versus temperature for stain-etched porous silicon. The lines represent the best fits of Eq. (5) to the data. Curves *a* and *b* show the best fits for the PL intensities of the two components obtained with 456-nm excitation. Curve *c* is the best fit for the PL intensity of the component obtained with 632-nm excitation.

blueshift of the PL spectrum with increase in temperature. Due to a stronger temperature dependence of the low-energy component (lower value of T_0), this component quenches faster than the high-energy component and this gives the appearance of a blueshift.

C. Nanosecond photoluminescence decays

The PL decays in *p*-Si have been reported^{22,23} to span a wide range of time scales from picoseconds to milliseconds. We found that the PL decays in stain-etched *p*-Si mainly spanned the range from nanoseconds to microseconds. The PL decays were recorded on a 0.1–50-ns time scale. As reported by previous workers,²² we also found that the PL decay cannot be fitted with a single-component exponential decay. Figure 5 shows the measured and fitted PL decay of a stain-etched film at an emission wavelength of 700 nm at 25 K with 373-nm excitation along with the weighted residuals for the fit. The instrument response is also shown in the curve. The randomness of the weighted residuals shows that the fit is excellent over the entire data set. The resulting lifetime distribution (Fig. 6) shows that there are two short lifetimes and a broad spread of lifetimes in the range greater than 30 ns. The peak of this slow-component distribution for stain-etched *p*-Si appears to be around 50–100 ns, which is considerably shorter than 100 μ s to 1 ms for anodically etched *p*-Si.^{13,18}

In order to study the two short lifetimes in the lifetime distribution in more detail, we decided to fit the PL decay

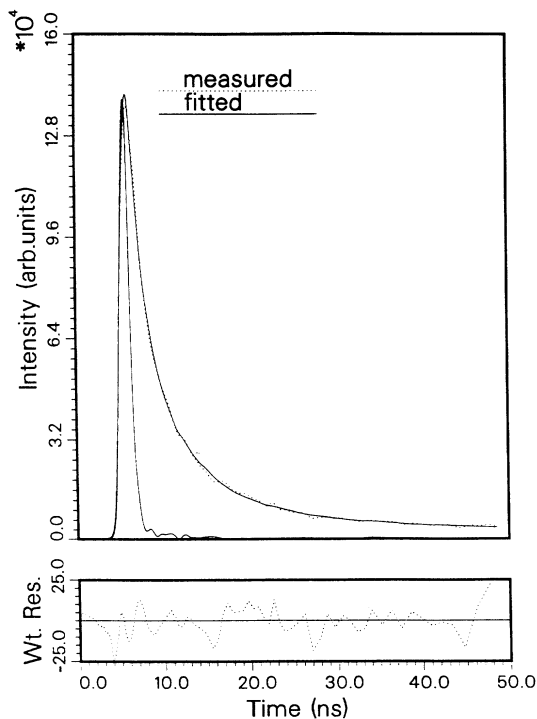


FIG. 5. Measured and fitted PL decay of stain-etched *p*-Si at an emission wavelength of 700 nm at 25 K with 373-nm excitation along with the weighted residuals for the fit. The instrument response is also shown.

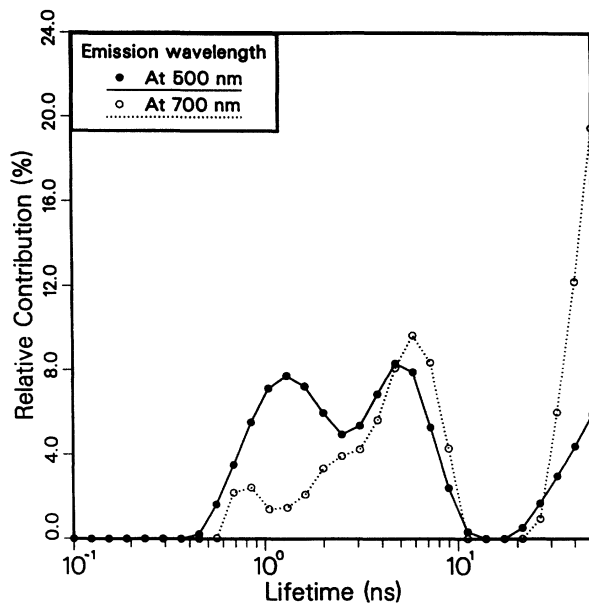


FIG. 6. Lifetime distributions of stain-etched *p*-Si at 500 and 700 nm at 25 K with 373-nm excitation.

with

$$I(t) = a_1 \exp(-t/\tau_1) + a_2 \exp(-t/\tau_2) + a_3 \exp(-t/\tau_3), \quad (2)$$

where τ_1 , τ_2 , and τ_3 are the decay times of the three components, and a_1 , a_2 , and a_3 are the corresponding pre-exponential factors. The third exponential in Eq. (2) is supposed to represent an average of the long lifetimes (> 30 ns) in the range 0.1–50.0 ns. Hence, the corresponding lifetime is not very significant, but the relative contribution is significant in further discussions.

Table I gives a summary of experimental parameters along with the decay times, percentage contributions, and fractional intensities of the components obtained by analyzing the PL decay curves using Eq. (2). For clarity, some of the values are repeated and grouped such that it is easy to identify the dependence of lifetimes and percentages upon emission energy, excitation energy, and temperature, respectively. For comparing the fractional intensities at 25 and 293 K, the decays were recorded under identical experimental conditions at the two temperatures. With 373-nm excitation, the decay times obtained for the two short components are 1.1 ± 0.1 and 4.9 ± 0.3 ns, respectively, at all three emission wavelengths. The relative contribution of the second component does not change much with emission wavelength, but the contribution of the first component decreases while that of the third component increases with an increase in emission wavelength. This suggests that the first and the third component are related while the second component has a different origin. When the excitation is changed from 373 to 540 nm, the PL decay at 700 nm is dominated by the second component and the contribution from the first and the third components to the decay is negligible. So a low-energy excitation effectively excites only the second

TABLE I. Summary of fitting results.

Excitation wavelength (nm)	Emission wavelength (nm)	Temperature (K)	τ_1 (ns)	P_1 (%)	I_1 (arb. units)	τ_2 (ns)	P_2 (%)	I_2 (arb. units)	P_3 (%)	I_3 (arb. units)
373	500	25	1.03	41.2		4.57	41.1		17.7	
373	600	25	1.23	24.5		5.00	47.8		27.7	
373	700	25	1.04	18.7	27.97	5.21	42.4	63.44	38.9	58.20
373	700	25	1.04	18.7	27.97	5.21	42.4	63.44	38.9	58.20
540	700	25	1.07	7.5	6.16	3.95	90.2	73.74	2.3	1.91
373	700	25	1.04	18.7	27.97	5.21	42.4	63.44	38.9	58.20
373	700	293	0.71	23.3	12.44	4.11	20.7	11.05	56.0	30.0
540	700	25	1.07	7.5	6.16	3.95	90.2	73.74	2.3	1.91
540	700	293	0.62	11.2	1.80	4.13	79.8	12.77	9.0	1.45

component of the decay. This can be correlated with the cw spectra in which the low-energy excitation excites only the second PL band. Thus, the second component of the decay relates to the cw PL band with an emission peak at 780 nm, while the first and the third components of the decay correspond to the high-energy band in the PL spectrum, which peaks at 700 nm. This is supported by the temperature dependence of the PL decay. The PL decay at 25 and 293 K was compared at 700 nm. With an increase in temperature, the PL decay intensity and the decay times decreased for 373-nm excitation. The percentage contributions of the first and the third components increased, whereas the contribution of the second component decreased. With an increase in temperature, the fractional intensities of the first and the third components decreased by approximately a factor of 2, whereas for the second component, the decrease was by a factor of 6. This change in fractional intensity for the second component agrees well with the temperature dependence of the cw PL intensity for the band which peaks at 780 nm, while the change in fractional intensity of the first and the third components agrees with the temperature dependence of the cw PL intensity for the band which peaks at 700 nm. This supports the earlier correlation of the second decay component with the low-energy cw PL band and that of the first and the third decay components with the high-energy cw PL band. With 540-nm excitation, the fractional intensity changes for the first and the third decay components are not very reliable because of very small percentage contributions at both temperatures. With 373-nm excitation, the temperature dependence of the lifetimes is much weaker than the temperature dependence of the PL intensity. This suggests that, with an increase in temperature, due to an increase in the available thermal energy, most of the carriers can find new states in which they recombine nonradiatively on a noncompeting time scale.

IV. DISCUSSION

The similarity between the ir spectra of stain-etched *p*-Si and anodically etched *p*-Si shows that the absorbing species in *p*-Si prepared by these two techniques are the same, but their relative concentrations are different. The

presence of additional oxygen-related peaks at 2240 and 860 cm^{-1} as well as the absorption band in the 1000–1200- cm^{-1} region indicate that the oxygen content in the stain-etched *p*-Si films is higher than in anodically etched *p*-Si films. As suggested by Brandt *et al.*,³ the peaks match very closely to those seen in the ir absorption spectra of siloxene molecules. Due to the absence of the O-H stretch absorption, we conclude that the number of O-H bonds in as-prepared stain-etched *p*-Si films is not very large. This suggests that stain-etched *p*-Si mainly consists of siloxene structures in which there is no significant substitution of H by O-H. The bonds which are not saturated by hydrogen probably remain as dangling bonds, serving as efficient nonradiative-recombination centers.

The cw PL spectra of stain-etched *p*-Si exhibit a two-band structure with high-energy excitation, with one band which peaks at 700 nm and another band which peaks at 780 nm. The similarity of these bands to those seen in annealed siloxene compounds further supports the presence of similar bonding in stain-etched *p*-Si. The excitation characteristics of these two bands agree with those reported by Stutzmann *et al.*¹³ in siloxene compounds. The functional form of the temperature dependence of the two bands is similar to that reported in siloxene compounds,²¹ but the extracted values of characteristic temperatures (T_0) are smaller in stain-etched *p*-Si. This suggests that the *p*-Si structure is more like an amorphous alloy of Si:O:H in which different clusters have bonding similar to that in the structural phases of siloxene.

The mechanism of radiative recombination in siloxene is not well known. Hirabayashi and Morigaki²⁴ have reported that as-prepared siloxene shows two components in the PL decay—a fast component in the region < 100 ns and a low component in the region $100 \text{ ns} < t < 50 \mu\text{s}$. They have also reported that on annealing the siloxene in vacuum at 350 °C, the slow component in the PL decay disappeared.²⁴ The lifetime distribution that we obtain for stain-etched *p*-Si seems to be between the lifetime distributions of as-prepared and annealed siloxene phases, but closer to the annealed siloxene phase. Hirabayashi and Morigaki²⁴ have assigned the fast component to intramolecular recombination and the slow component to intermolecular recombination. We extend the same ideas

to *p*-Si and suggest that the faster components are due to highly localized electron-hole pairs and the slower components are from electron-hole pairs separated by larger distances.

There are two possibilities for the mechanism of recombination leading to slow decay. The slower-decay component may be due to band to band recombination with excess carrier densities strongly exceeding the equilibrium value.¹³ The intrinsic lifetime of the recombination process in this case can be long, because the band-to-band recombination occurs within an indirect band gap.¹⁷ The radiative rate may be determined by the intrinsic lifetime of excited states within the silicon rings in siloxene structures and the rate at which excited carriers can be transferred from other parts of the network into these rings.³ This gives rise to a broad distribution of lifetimes. The second possibility could be that the slow decay arises from radiative tunneling recombination as proposed in *a*-Si:H.²⁰ The broad distribution of lifetimes in this case indicates a broad distribution of separations between the recombining holes and electrons.

The overall lifetime distribution in stain-etched *p*-Si shorter than that reported in anodically etched *p*-Si,¹³ but agrees better with the siloxene lifetime distribution.²⁴ The average quantum efficiency of stain-etched *p*-Si is smaller than of anodically etched *p*-Si. We attribute this to an increase in nonradiative recombination due to an increase in the density of recombination centers such as dangling bonds. On annealing as-prepared siloxene, such an increase in the density of dangling-bond centers has been reported²⁵ by ESR measurement. This increase in siloxene has been attributed to destruction of the silicon layer structure by cross linking and dehydrogenation. There is a good possibility that similar structural changes result in higher dangling-bond density in stain-etched *p*-Si. Optically detected magnetic resonance results in anodically etched *p*-Si support¹³ the idea that the nonradiative recombination is via dangling bonds with at least one oxygen neighbor. The measured lifetime for competing radiative and nonradiative processes is given by

$$\frac{1}{\tau} = \frac{1}{\tau_r} + \frac{1}{\tau_{nr}}, \quad (3)$$

where τ_r and τ_{nr} are the radiative and nonradiative decay time, respectively. So if $\tau_{nr} \ll \tau_r$, then there will be a quenching of the PL efficiency accompanied by a shortening of the measured lifetime. This explains why the PL efficiency of stain-etched films is smaller than of anodically etched films, and the lifetime distribution in the

microsecond-millisecond time range is quenched to the nanosecond-microsecond range.

If the origin of the first- and the slow-decay component is the same, then Eq. (3) suggests that a fast nonradiative transition competing with the slow-decay component may be responsible for such a short measured lifetime. Matsumoto *et al.*²² have reported decay times of 0.16 and 0.38 ns in anodically etched *p*-Si, which are even shorter than the ones we see. We think that in the overall lifetime distribution these components are very weak and arise from fast nonradiative processes competing with slow radiative processes. The second decay component is excited efficiently at 2.3 eV and can be correlated with the low-energy component of the cw PL. It is possible that as proposed in siloxene²⁴ this component has an excitonic origin characteristic of a Frenkel exciton. The strong localization of electrons and holes occurring due to siloxene-type bonding, and a smaller refractive index, may be responsible for the excitonic recombination. The corresponding peak in the cw PL spectrum is probably broadened by the disorder present in the material.

V. CONCLUSIONS

In conclusion, we have characterized stain-etched *p*-Si by means of ir absorption spectra, cw PL spectra, and nanosecond PL decay. We are able to correlate these results very well with each other. From the correlation the following understanding emerges: Stain-etching of *c*-Si with HF:HNO₃:H₂O produces an amorphous alloy of silicon, oxygen, and hydrogen in which the bonding configuration is very similar to that of annealed siloxene at various places. The stain-etched *p*-Si mainly consists of siloxene phases which do not have direct O-H bonding. The as-prepared stain-etched *p*-Si films have a very high density of dangling bonds, which act as effective recombination centers and reduce the quantum efficiency of stain-etched *p*-Si. The different siloxene phases give rise to cw PL spectra with two bands with distinct temperature dependences and excitation characteristics. The nanosecond PL decays in stain-etched *p*-Si show the presence of fast as well as slow components, similar to PL decay in siloxene.

ACKNOWLEDGMENTS

We would like to thank Dr. Borst and A. Kher for the development of the lifetime-fitting program. We would also like to thank Dean Stubbs for building the etch cell.

¹L. T. Canham, Appl. Phys. Lett. **57**, 1046 (1990).

²V. Lehmann and U. Gösele, Appl. Phys. Lett. **58**, 856 (1991).

³M. S. Brandt, H. D. Fuchs, M. Stutzmann, and M. Cardona, Solid State Commun. **81**, 307 (1992).

⁴R. Sabet-Darmani, D. Haneman, A. Hoffman, and D. D. Cohen, J. Appl. Phys. **73**, 2321 (1993).

⁵M. A. Tischler, R. T. Collins, J. H. Stathis, and J. C. Tsang, Appl. Phys. Lett. **60**, 639 (1992).

⁶R. W. Fathauer, T. George, A. Ksendzov, and R. P. Vasquez, Appl. Phys. Lett. **60**, 995 (1992).

⁷R. P. Vasquez, R. W. Fathauer, T. George, and A. Ksendzov, Appl. Phys. Lett. **60**, 1004 (1992).

⁸C. Palsule, S. Gangopadhyay, A. Kher, W. Borst, U. Schmidt, B. Schehr, and B. Schröder, Phys. Rev. B **47**, 9309 (1993).

⁹D. R. James and W. R. Ware, Chem. Phys. Lett. **126**, 7 (1986).

¹⁰J. M. Lavine, S. P. Sawan, T. Shieh, and A. J. Bellezza, Appl.

- Phys. Lett. **62**, 1099 (1993).
- ¹¹C. Tsai, K. H. Li, D. S. Kinosky, R. Z. Qian, T. C. Hsu, J. T. Irby, S. K. Banerjee, A. F. Tasch, J. C. Campbell, B. K. Hance, and J. M. White, *Appl. Phys. Lett.* **60**, 1700 (1992).
- ¹²H. D. Fuchs, M. Stutzmann, M. S. Brandt, M. Rosenbauer, J. Weber, A. Breitschwerdt, P. Deák, and M. Cardona, *Phys. Rev. B* **48**, 8172 (1993).
- ¹³M. Stutzmann, J. Weber, M. S. Brandt, H. D. Fuchs, M. Rosenbauer, P. Deák, A. Höpner, and A. Breitschwerdt, *Adv. Solid State Phys.* **32**, 179 (1992).
- ¹⁴H. Kautsky, *Z. Anorg. Chem.* **117**, 209 (1921).
- ¹⁵F. Wöhler, *Lieb. Ann.* **127**, 275 (1863).
- ¹⁶M. Stutzmann, M. S. Brandt, M. Rosenbauer, J. Weber, and H. D. Fuchs, *Phys. Rev. B* **47**, 4806 (1993).
- ¹⁷P. Deak, M. Rosenbauer, M. Stutzmann, J. Weber, and M. S. Brandt, *Phys. Rev. Lett.* **69**, 2531 (1992).
- ¹⁸C. Wang, J. M. Perz, F. Gaspari, M. Plumb, and S. Zukotynski, *Appl. Phys. Lett.* **62**, 2676 (1993).
- ¹⁹M. Kastner, *J. Phys. C* **13**, 3319 (1980).
- ²⁰R. A. Street, *Adv. Phys.* **30**, 593 (1981).
- ²¹I. Hirabayashi, K. Morigaki, and S. Yamanaka, *J. Phys. Soc. Jpn.* **52**, 671 (1983).
- ²²T. Matsumoto, M. Daimon, T. Futagi, and H. Mimura, *Jpn. J. Appl. Phys.* **31**, L619 (1992).
- ²³G. W. 't Hooft, Y. A. R. R. Kessener, G. L. J. A. Rikken, and A. H. J. Venhuizen, *Appl. Phys. Lett.* **61**, 2344 (1992).
- ²⁴I. Hirabayashi and K. Morigaki, *J. Non-Cryst. Solids* **59&60**, 645 (1983).
- ²⁵H. Ubara, T. Imura, A. Hiraki, I. Hirabayashi, and K. Morigaki, *J. Non-Cryst. Solids* **59&60**, 641 (1983).